



Proceedings of the Seventeenth International Conference on  
Civil, Structural and Environmental Engineering Computing  
Edited by: P. Iványi, J. Kruis and B.H.V. Topping  
Civil-Comp Conferences, Volume 6, Paper 4.4  
Civil-Comp Press, Edinburgh, United Kingdom, 2023  
doi: 10.4203/ccc.6.4.4  
©Civil-Comp Ltd, Edinburgh, UK, 2023

## **Measurement of the density of formed structures for concrete 3D printing**

**Z.B. Zuo<sup>1,2</sup>, W. De Corte<sup>1</sup>, Y.L. Huang<sup>2</sup>, L.L. Zhang<sup>2</sup>,  
J. Li<sup>3</sup> and Y. Yuan<sup>4</sup>**

**<sup>1</sup>Faculty of Engineering and Architecture, Ghent University,  
Ghent, Belgium**

**<sup>2</sup>General Engineering Institute of Shanghai Construction Group,  
Shanghai Construction Group Co., Ltd., Shanghai, China**

**<sup>3</sup>Nanjing KENYO Digital Material Technology Research  
Institute Co., Ltd., Nanjing, China**

**<sup>4</sup>State Key Laboratory of Disaster Reduction in Civil  
Engineering, Tongji University, Shanghai, China**

### **Abstract**

As one of the core parameters of three-dimensional (3D) printing, the density of formed structures directly governs the quality and performance of printed buildings or components. Therefore, it is critical to measure the density during printing. Here, we propose a density measurement system (DMS) and computational method for formed structures during concrete 3D printing (C3DP). The DMS includes a real-time weight monitoring system and software, and a 3D laser scanning system for measuring the volume of the formed structures. The corresponding method introduces parameters such as printing time, mass printing speed and relative density. Several 3D printing indoor experiments were conducted to illustrate the DMS and method. Experimental results show that the density of the formed structures during 3D printing can be measured quickly, quantitatively and with high accuracy. The density of the formed structures ranged from 2016 to 2179 kg/m<sup>3</sup>, with an average value of 2068 kg/m<sup>3</sup>. These results can provide a basis for evaluating the uniformity and quality of formed structures, as well as support the monitoring and feedback control of the process parameters during 3D printing, including printing time gap, printing speed, and mass printing speed.

**Keywords:** concrete 3D printing, formed structures, density, experimental device, calculation method, measurement method

## 1 Introduction

Three-dimensional (3D) printing, as an emerging technology that allows for the fully automated manufacturing [1] of complex, personalized products directly from digital models, promises to change the current modes of construction [2].

Concrete 3D printing (C3DP) is a layer-by-layer forming process without formwork. The printing process is non-linear [3] and mostly without vibration. Furtherly, the density of the formed structure inevitably deviates from the design density. If the density deviation is too large, it directly affects the safety of formed structures during printing as well as the quality [4] and performance (e.g., thermal conductivity, mechanical properties, and durability [5]) of the final hardened 3D printed building or component. Therefore, it is critical to measure and control the density of formed structures during printing. In recent years, many scholars have studied this aspect. Du et al. [6] studied the effect of particle size distribution on sintered density and density of a densely packed powder during binder jetting printing. Ali et al. [4] developed a methodology based on nano-computed tomography for measuring the relative powder-bed compaction density in powder-bed printing processes. Li et al. [7] measured and calibrated the density of selective laser sintered printing powder bed based on the plumb bob method. Toprak et al. [3] used neuro-fuzzy modelling methods to predict the relative density of stainless steel 316L metal parts produced by 3D printing. Tanlak et al. [8] utilized computerized numerical methods to predict the range of printable densities of lattice structures. Liu et al. [9] investigated the effect of infill density on the performance of 3D-printed robotic grippers through numerical simulations and experiments. Ramakrishnan et al. [10] proposed a C3DP approach based on hollow-core extrusion to reduce the density of printed elements and thus improve the thermal performance of the printed lightweight structures.

Since C3DP is a complex dynamic forming process, the self-weight of the post-printed layer structure causes deformation of the already-printed layer structure. Therefore, there is still a huge challenge of measuring and controlling the density of formed structures for C3DP. The main objective of this paper is to investigate the methodology used to measure the density of formed structures during C3DP.

## 2 Methods

### 2.1 Experimental device

A density measurement system (DMS) for formed structures suitable for C3DP was developed, as shown in Figure 1. The DMS includes a weight monitoring system, a 3D laser scanning system and a computer. The weight monitoring system is designed and manufactured to monitor the weight of the formed structure in real-time during the 3D printing deposition process, which includes a bearing platform supporting the formed structure, four weighing sensors connected to the lower surface of the bearing

platform, four auto-leveling bases mounted at the bottom of the weighing sensors, a data acquisition connected to the weighing sensors, and a real-time weight monitoring software. The bearing platform is made of transparent tempered glass. The maximum range of a single weighing sensor is 50 kg and the excitation voltage is 5-12 V. A 3D laser scanner Z + F imager 5010 is adopted to measure the volume of the formed structures. The measurement range is 0.3-187.3 m, the maximum scanning rate is 1,016,000 points/s, the scanning angle is 320×360 degrees, the measurement resolution is 0.1 mm, and the linear accuracy is 1 mm at a distance of 50 m [2]. The softwares JRC 3D reconstructor and Geomagic control were adopted for the corresponding data post-processing. In addition, a 3D printer was used to print test samples of concrete structures. The length, width and height of the printer are 4.2 m, 4 m and 4 m, respectively. The diameters of the available printing heads are in 20 mm and 40 mm, the printing speed is 0-0.25 m/s and the positioning accuracy is 1 mm.

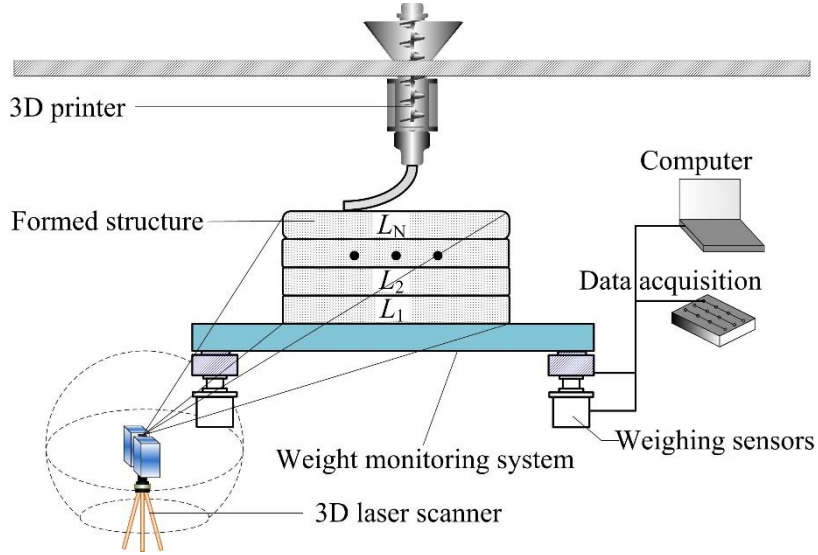


Figure 1: Density measurement system for formed structures during 3D printing.

## 2.2 Computational method

The density  $\rho_t$  of the formed structure at time  $t$  during 3D printing deposition can be calculated by the following equation.

$$\rho_t = \frac{m_t}{V_{t+\delta}} = \frac{\sum_{i=1}^{n_W} m_{ti}}{V_{t+\delta}} \quad (1)$$

where  $m_t$  is the mass of the formed structure monitored by the weight monitoring system at time  $t$ , and the unit is kg.  $m_{ti}$  is the mass of the formed structure monitored by the  $i$ -th weighing sensor at  $t$ , and the unit is kg.  $n_W$  is the total number of weighing sensors.  $\delta$  is the time period required for 3D scanning the structure, and it is assumed that the deformation of the formed structure during time period  $\delta$  is negligible.  $V_{t+\delta}$  is the volume of the formed structure obtained by 3D laser scanning after stopping printing at time  $t$  and  $\delta$ , and the unit is  $\text{m}^3$ . It is assumed here that the clearance inside the formed structure is negligible.

### 2.3 Test methods

Several indoor experiments for density measurements of formed structures were conducted using specimens (Figure 2) with dimensions of  $0.15 \times 0.15 \times 0.15$  m, as shown in Figure 3. The material used for the 3D printing tests consisted of cement (42.5 grade Poland cement), water, sand, additives and polypropylene fiber. The ratio of sand to cement per cubic meter of the material is approximately 1.5. Depending on the size and material of the 3D printing of specimens, the appropriate process parameters were set for the 3D printer. The diameter of the printing head is selected to be 20 mm, the layer width  $\omega$  is 25 mm, the layer resolution  $\delta$  is 10 mm, the printing path is of the rectangular rotate type [11], the printing path length  $L_p$  of a single printing layer is approximately 0.875 m, the number of printing layers  $N_L$  is 10, the printing speed  $v$  is 0.1 m/s, and the printing time gap  $t_g$  is 8.6 s. The data acquisition frequency of the weight monitoring system is 30 Hz.  $\delta$  of the 3D laser scanning is 1010 s after 10 printing layers are printed.

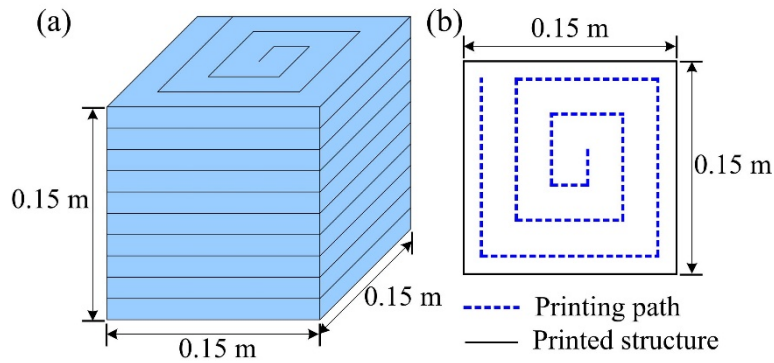


Figure 2: A 3D printing of specimen for density measurement laboratory tests. (a) Specimen and dimensions. (b) Rectangular rotating printing path.

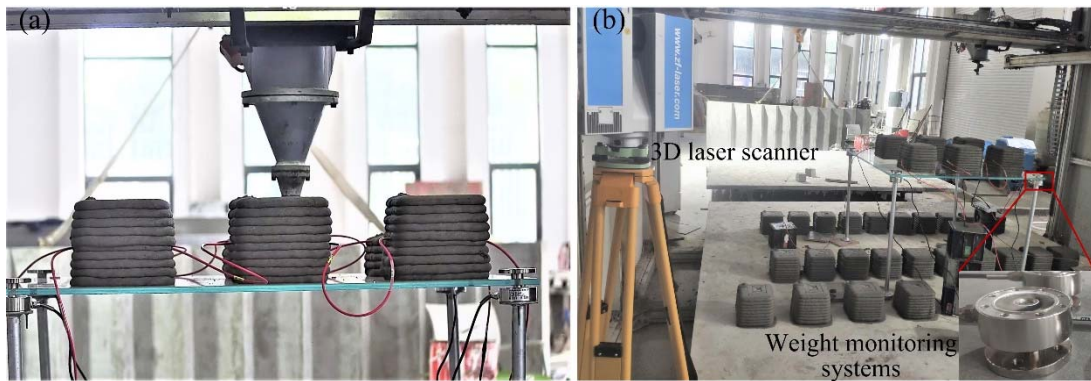


Figure 3: Indoor experiments for density measurement of representative 3D printing of formed structures. (a) 3D printed specimens and monitoring of the weight of formed structures. (b) 3D scanning of formed structures.

The number of 3D printing of concrete specimens is 6, numbered S1, S2, S3, S4, S5 and S6, and the scheme of the test is as follows. Concrete specimens were sequentially printed on the bearing platform supporting the formed structure, and five printing layers were completed, with the printed specimens numbered S1-0.5, S2-0.5,

S3-0.5, S4-0.5, S5-0.5, and S6-0.5, in that order. Concrete specimens were continued to be printed sequentially and five printing layers were completed with the printed specimens numbered S1-1, S2-1, S3-1, S4-1, S5-1 and S6-1 in that order, and the printing of specimens S1-S6 was finalized for the tests.

### 3 Results and Discussion

Figure 4 shows the mass of the formed structures at different times monitored by the weight monitoring system during printing. In the case of specimen S1-0.5, the number of layers formed during 3D printing extrusion increases with time  $t$ , and  $m_t$  monitored by the weight monitoring system increases as well. When the specimen S1-0.5 finishes printing, the printing head stops extruding and the printing head moves to the position where the specimen S2-0.5 is to be printed, and  $m_t$  remains constant during this period. Different specimens have different printing stopping times or printing head moving (stopping extrusion) times, but  $m_t$  and  $t$  show a similar law during printing. The value of  $m_t$  is linearly related to  $t$  throughout the printing test (printing process for all specimens). The law can be summarized in the following equation.

$$m_t = \begin{cases} v_{ma}t + m_a & 0 \leq t \leq t_a \\ v_{mj}t + m_j & 0 \leq t \leq \Delta_{ij} \\ 0 & 0 \leq t \leq \Psi_{ij} \end{cases}, v_{ma} \leq v_{mj} \quad j = 1, 2, \dots, 6 \quad (2)$$

where  $j$  is the printing of the  $j$ -th specimen.  $t_a$  is the total time in the entire printing test, and the unit is s.  $v_m$  is the mass of the 3D printing of formed structure per unit time, i.e., the mass printing speed, and the unit is kg/s.  $v_{ma}$  is the mass printing speed in  $t_a$ , and the unit is kg/s.  $m_a$  is the mass fitting coefficient at  $t_a$ , and the unit is kg.  $\Delta_{ij}$  is the printing time of the  $j$ th specimen, and the unit is s.  $v_{mj}$  is the mass printing speed of the  $j$ -th specimen at  $\Delta_{ij}$ , and the unit is kg/s.  $m_j$  is the mass fitting coefficient of the  $j$ -th specimen at  $\Delta_{ij}$ , and the unit is kg.  $\Psi_{ij}$  is the printing pause time from the  $j$ -th specimen to the  $(j+1)$ -th specimen ( $j$  takes the values 1, 2, ..., 5) or the travel time for the printing head (stop extrusion), and the unit is s. Since there is the time  $\Psi_{ij}$  throughout the printing process,  $v_{ma}$  is less than or equal to  $v_{mj}$ . The data for part of the time  $m_t$  in Figure 4 showed small up and down vibrations due to the external loads applied during this period. However, this does not affect the accuracy of equation (2).

Figure 4 also shows that the mass  $\Delta m_j$  and the printing time  $\Delta t_j$  of either printed specimen can be calculated by the weight monitoring system.

$$\Delta m_j = \text{MAX}(m_{ij}) - \text{MAX}(m_{i(j-1)}), \quad j = 1, 2, \dots, 6 \quad (3)$$

$$\Delta t_j = \text{MAX}(t_j) - \text{MIN}(t_j), \quad j = 1, 2, \dots, 6 \quad (4)$$

where  $\text{MAX}(m_{ij})$  is the stabilization value of the mass of the formed structure monitored by the weight monitoring system after reaching the maximum value during the printing of the  $j$ -th specimen, and the unit is kg.  $\text{MAX}(m_{i(j-1)})$  is the stabilization

value of the mass of the formed structure monitored by the weight monitoring system after reaching the maximum value during the printing of the  $(j-1)$ -th specimen ( $j$  takes the values 2, 3..., 6), and the unit is kg.  $\text{MAX}(t_j)$  is the time corresponding to when the mass of the formed structure, monitored by the weight monitoring system, reaches a stabilized value for the first time during the printing of the  $j$ -th specimen, and the unit is s.  $\text{MIN}(t_j)$  is the time corresponding to the time before the  $j$ -th specimen is printed, and before the first increase in the mass of the  $(j-1)$ -th specimen ( $j$  takes the values 2, 3..., 6), monitored by the weight monitoring system, after reaching a stabilized value.

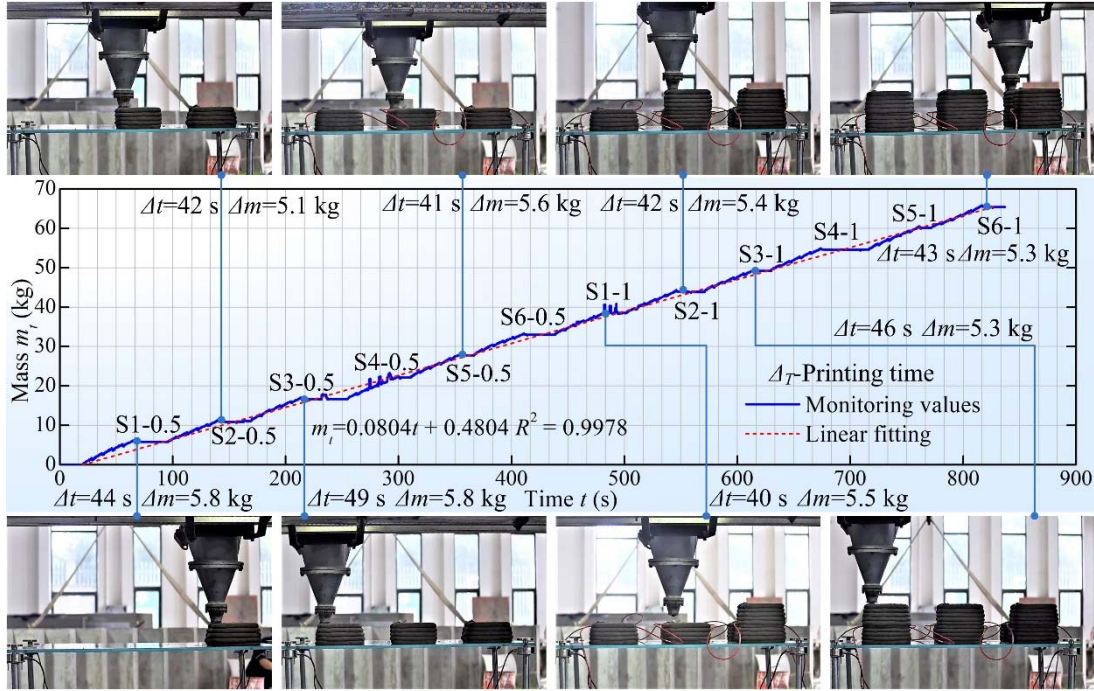


Figure 4: Mass of formed structures at different times monitored by the weight monitoring system during printing.

In addition, the printing time gap  $t_g$ , the printing speed  $v$  and the mass printing speed  $v_m$  can be calculated by the following equations.

$$t_g = \frac{\Delta t}{N_L} \quad (5)$$

$$v = \frac{L_p}{t_g} \quad (6)$$

$$v_m = \frac{\Delta m}{\Delta t} \quad (7)$$



According to equations (3)~(7),  $t_g$ ,  $v$  and  $v_m$  were calculated for different specimens as shown in Figure 5. The average value of  $t_g$  is 8.7 s, the average value of  $v$  is 0.101 m/s and the average value of  $v_m$  is 0.126 kg/s for the whole printing test.

Figure 6 shows the volume of 3D printing of formed structures measured by 3D laser scanning. The number of points of the scanned point cloud of specimens S1~S6 is 436125. The volume  $V$  of the formed structure of each 3D printed specimen was calculated according to the point cloud model, and the density  $\rho$  of the formed structure of each 3D printed specimen is calculated according to equation (1), as shown in Table 1. The average value of  $V$  is 0.005273 m<sup>3</sup>.  $\rho$  ranges from 2016 to 2179 kg/m<sup>3</sup>, and the average value is 2068 kg/m<sup>3</sup>.

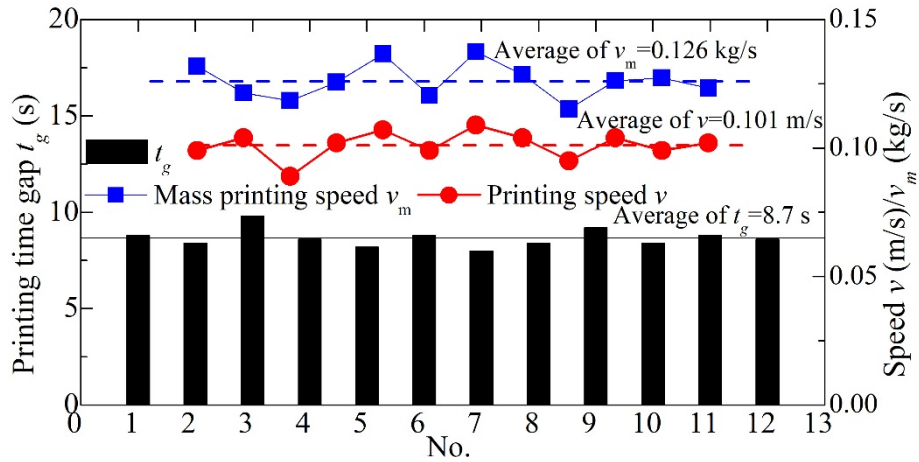


Figure 5: Printing time gap and speeds calculated based on the weight monitoring system.

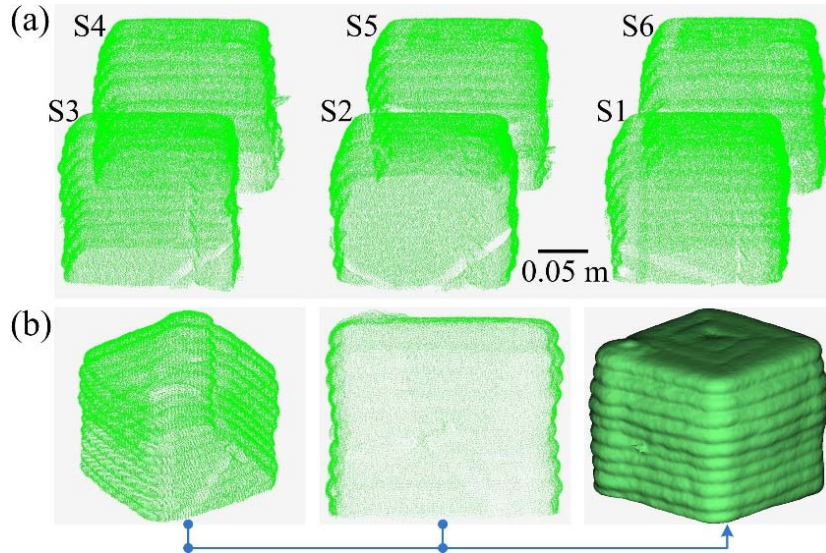


Figure 6: Volume of 3D printing of formed structures measured by 3D laser scanning. (a) Point cloud of 3D laser scanning. (b) Measurement of the volume of formed structures.

Specimen No.	Printing time [s]	Printing time gap [s]	Printing speed [mm/s]	Mass [kg]	Mass printing speed [kg/s]	Volume [m <sup>3</sup> ]	Calculated density [kg/m <sup>3</sup> ]
S1	84	8.4	0.104	11.30	0.135	0.005187	2178.52
S2	84	8.4	0.104	10.50	0.125	0.005145	2040.82
S3	95	9.5	0.092	11.10	0.117	0.005506	2015.98
S4	85	8.5	0.103	10.70	0.126	0.005189	2062.05
S5	85	8.5	0.103	11.20	0.132	0.005477	2044.92
S6	87	8.7	0.101	10.60	0.122	0.005133	2065.07

Table 1: Calculation of density of 3D printing of formed structures based on monitoring and scanning results.

The main contribution of this paper is to propose a novel system and calculation method for measuring the density of C3DP of forming structures, which realizes rapid, highly accurate and quantitative measurement of the density of the formed structure. The system and method can provide a basis for evaluating the uniformity and quality of formed structures, and support the monitoring and feedback of process parameters during printing. In order to further apply the DMS and calculation method, the rationality assessment method of the density of the formed structural layer  $L_N$  during printing was proposed, as shown in Figure 7, with the following steps.

- i) Adjust and control printing and material parameters.
- ii) Print layers  $L_1, L_2, \dots$  and  $L_N$  in sequence. iii) Monitor the mass  $m_N$  of the printed layer  $L_N$  using the weight monitoring system. iii) Measure the volume  $V_N$  of the printed layer  $L_N$  using the 3D scanning system. iv) Calculate the relative density  $I_N$  of layers  $L_1, L_2, \dots$  and  $L_N$  according to equation (8). v) Evaluate the reasonableness of the relative density of layers  $L_1, L_2, \dots$  and  $L_N$  according to equation (9). If equation (9) is satisfied, the printed layer  $L_N$  is feasible; if equation (9) is not satisfied, printing parameters and materials need to be adjusted and controlled for reprinting. Where  $a$  and  $b$  are the maximum and minimum values of the design relative density.

$$I_N = \frac{|\rho_s - m_N / V_N|}{\rho_s} \quad (8)$$

$$a \leq I_N \leq b \quad (9)$$



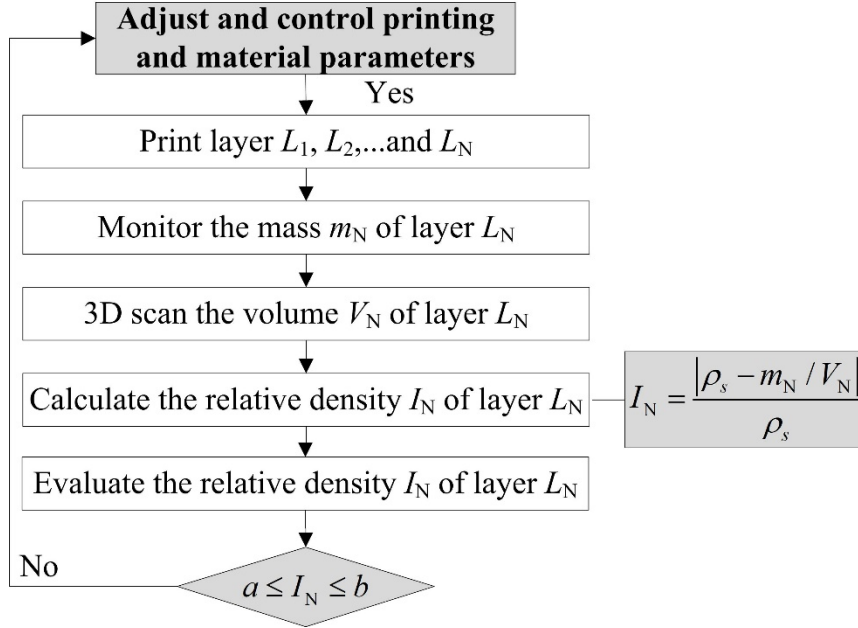


Figure 7: Rationality assessment of the density of formed layers during 3D printing.

#### 4 Conclusions and Contributions

In this work, A DMS and computational method of formed structures during C3DP is presented. The DMS includes a newly developed weight monitoring system and software that measures the weight of formed structures in real time, as well as a 3D laser scanning system for measuring the volume of formed structures. Moreover, the computational method of applying the DMS is proposed, and the corresponding method introduces parameters such as printing time, mass printing speed and relative density. Several 3D printing indoor experiments were carried out using the DMS. The test results show a linear increase in  $m_t$  with  $t$  throughout the printing test and during the printing of individual specimens, with  $v_{ma}$  less than or equal to  $v_{mj}$ . With the proposed DMS and the corresponding computational method, the density of formed structures during 3D printing can be measured quickly, quantitatively and with high accuracy. In these tests,  $\rho$  ranges from 2016 to 2179 kg/m<sup>3</sup>, and the average value is 2068 kg/m<sup>3</sup>. Process parameters during 3D printing can be calculated with feedback. Hence, the average value of  $t_g$  is 8.7 s, the average value of  $v$  is 0.101 m/s and the average value of  $v_m$  is 0.126 kg/s for the whole printing test.

The system and method proposed in this paper can provide a basis for evaluating the uniformity and quality of formed structures, as well as support the monitoring and feedback control of process parameters during 3D printing, which can help to improve the precision and quality of concrete 3D printing.

#### Acknowledgements

This work is financially supported by the National Key R&D Program of China (No. 2018YFC0705800) and the Science and Technology Commission of Shanghai

Municipality (No. 19QB1403300). We thank D. Chen of Shanghai Construction Group, Z.J. Duan of Nanjing KENYO, and W. Chen of Southeast University for their help in preparing the experiments.

## References

- [1] V. Mechtcherine, V.N. Nerella, F. Will, M. Näther, J. Otto, M. Krause, "Large-scale digital concrete construction – CONPrint3D concept for on-site, monolithic 3D-printing", *Automation in Construction*, 107: 102933, 2019, doi: 10.1016/j.autcon.2019.102933.
- [2] Z.B. Zuo, J. Gong, Y.L. Huang, Y.J. Zhan, M. Gong, L.L. Zhang, "Experimental research on transition from scale 3D printing to full-size printing in construction", *Construction and Building Materials*, 208: 350–360, 2019, doi: 10.1016/j.conbuildmat.2019.02.171.
- [3] C.B. Toprak, C.U. Dogruer, "Neuro-fuzzy modelling methods for relative density prediction of stainless steel 316L metal parts produced by additive manufacturing technique", *Journal of Mechanical Science and Technology*, 37(1), 107–118, 2023, doi: 10.1007/s12206-022-1211-6.
- [4] U. Ali, Y. Mahmoodkhani, S. Imani Shahabad, R. Esmaeilzadeh, F. Liravi, E. Sheydaeian, K.Y. Huang, E. Marzbanrad, M. Vlasea, E. Toyserkani, "On the measurement of relative powder-bed compaction density in powder-bed additive manufacturing processes", *Materials and Design*, 155: 495–501, 2018, doi: 10.1016/j.matdes.2018.06.030.
- [5] D. Talke, B. Saile, N. Meier, F. Herding, I. Mai, H. Zetzener, A. Kwade, D. Lowke, "Particle-bed 3D printing by selective cement activation – Influence of process parameters on particle-bed density", *Cement and Concrete Research*, 168: 107140, 2023, doi: 10.1016/j.cemconres.2023.107140.
- [6] W. Du, J. Roa, J. Hong, Y. Liu, Z. Pei, C. Ma, "Binder jetting additive manufacturing: Effect of particle size distribution on density", *Journal of Manufacturing Science and Engineering*, 143(9): 091002, 2021: doi: 10.1115/1.4050306.
- [7] J. Li, G. Gao, S. Zhang, Y. Du, "Calibration and measurement study on density of selective laser sintered 3D printing powder bed", *Journal of Physics: Conference Series*, 1267: 012072, 2019, doi: 10.1088/1742-6596/1267/1/012072.
- [8] N. Tanlak, D.F. De Lange, W. Van Paepegem, "Numerical prediction of the printable density range of lattice structures for additive manufacturing", *Materials and Design*, 133: 549–558, 2017, doi:10.1016/j.matdes.2017.08.007.
- [9] C.-H. Liu, P.-T. Hung, "Effect of the infill density on the performance of a 3D-printed compliant finger", *Materials and Design*, 223: 111203, 2022. doi: 10.1016/j.matdes.2022.111203.
- [10] S. Ramakrishnan, S. Muthukrishnan, J. Sanjayan, K. Pasupathy, "Concrete 3D printing of lightweight elements using hollow-core extrusion of filaments", *Cement and Concrete Composites*, 123: 104220, 2021, doi: 10.1016/j.cemconcomp.2021.104220.

- [11] Z. Pan, D. Si, J. Tao, J. Xiao, "Compressive behavior of 3D printed concrete with different printing paths and concrete ages", *Case Studies in Construction Materials*, 18: e01949, 2023, doi: 10.1016/j.cscm.2023.e01949.